J Mater Sci: Mater Med (2010) 21:1875–1880
DOI 10.1007/s10856-010-4038-0

Hydroxyapatite nanoparticles as a controlled-release carrier of BMP-2: absorption and release kinetics in vitro

Guangping Xie · Jiao Sun · Gaoren Zhong · Changsheng Liu · Jie Wei

Received: 5 February 2009 / Accepted: 23 February 2010 / Published online: 19 March 2010

Abstract Recently, nanoparticles have been extensively developed as controlled-release carriers; however, there has been little research on hydroxyapatite nanoparticles (HANPs) and their potential applications. In this study, HANPs were investigated as a controlled-release carrier of bone morphogenetic protein-2 (BMP-2), the absorption and release kinetics of which were analyzed in vitro. Different concentrations of BMP-2 solution were used to evaluate the adsorptive properties of HANPs. It was observed that the amount of BMP-2 adsorbed onto HANPs could be as high as 70 μg/mg and that adsorption rate was highly correlated with the concentration of BMP-2 solution used. After absorption, the suspension of HANPs absorbed BMP-2 (HANPs/BMP-2) was incubated at 37°C for 15 days and the release kinetics of BMP-2 from HANPs/BMP-2 was determined daily. The release profile showed sustained release of BMP-2 over the period of the investigation. Collectively, these results suggest that HANPs has the potential to function as a carrier for drug delivery systems and as a scaffold material in bone tissue engineering.

G. Xie · J. Sun (✉)
Shanghai Biomaterials Research & Testing Center, Shanghai Ninth People's Hospital, Shanghai JiaoTong University School of Medicine, 200011 Shanghai, China
e-mail: jiaosun59@yahoo.com

G. Zhong
School of Pharmacy, Fudan University, 200037 Shanghai, China

C. Liu · J. Wei
School of Materials Science and Engineering, East China University of Science and Technology, 200237 Shanghai, China

1 Introduction

Hydroxyapatite [$Ca_{10}(PO_4)_6(OH)_2$; HA], the main mineral component of bones and teeth, is well known for its high biocompatibility, osteoconductivity, and osteoinductivity [1, 2]. Artificially synthesized HA particles have been used extensively for bone repair and tissue engineering [3, 4], and have also been utilized as an adsorbent material for chromatographic purification and separation owing to their excellent capability of adsorbing many molecules [5–7]. It has also been reported that HA particles reversibly adsorb many chemicals and proteins [8, 9], suggesting that they would be suitable as carriers of drugs. Ono et al. used HA particles as protein carriers, and demonstrated that proteins were well absorbed onto the HA particles but also that they were rapidly released from these particles in vitro [10]. Nevertheless, the speed at which the proteins are released from HA particles is unsatisfactory and this has become an important challenge in the application of these materials as drug delivery systems (DDS).

The application of nanotechnology to biomedical research is expected to have a major impact leading to the development of new types of diagnostic and therapeutic tools. One focus in nanobiotechnology is the development of safe and efficient drug/gene delivery vehicles [11]. Recently, nanoparticles (NPs) have been developed extensively as drug carriers owing to their small size and good penetrability in the body [12]. HA nanoparticles (HANPs) is a type of inorganic NP that not only has the specific properties of NPs, such as small size and large surface area, but also possesses superior bioactivity compared with HA micron-size particles [13, 14]. Nevertheless, despite of these properties, HANPs has received little attention in the field of controlled-release carriers in DDS.

Bone morphogenetic protein-2 (BMP-2), a growth factor that induces the differentiation of osteoprogenitor cells into osteoblasts and influences bone pattern formation, has been extensively used in bone tissue engineering [15, 16]. During the process of bone formation, continuous release of BMP-2 is extremely important [17]. To this end, scaffold materials have also been designed as carriers to convey and release BMP-2 in bone tissue engineering. In the past few years, a variety of scaffold materials including hydroxyapatite and tricalcium phosphate have been used in bone tissue engineering as carriers of BMP-2 [18, 19]. However, there have been no reports of HANPs being designed as a carrier to carry and controllably release BMP-2 in bone tissue engineering.

In view of this deficiency, HANPs were investigated in this study as protein carriers and the absorption and release kinetics of proteins in vitro were analyzed. BMP-2 was selected as the model growth factor protein in the investigation. The amounts of BMP-2 that could absorb onto HANPs using different concentrations of BMP-2 solution and the subsequent release of absorbed BMP-2 over time were examined. In order to precisely quantify the amounts of BMP-2 involved, BMP-2 was radiolabeled with ^{125}I on account of the high sensitivity of radioassay.

2 Materials and methods

2.1 Reagents

All the chemicals used were of analytical reagent grade. Calcium nitrate [$Ca(NO_3)_2$], ammonium hydrogen phosphate [$(NH_4)_2HPO_4$], hydrochloric acid (37%), and ammonia (25%) were purchased from Sinopharm Chemical Reagent Co., Ltd. (China). Sodium iodide ($Na^{125}I$) was a product from the China Institute of Atomic Energy. BMP-2 was purchased from Guangzhou Dahui Biotechnology Co., Ltd. (China). Iodogen and Sephadex columns were obtained from Sigma (USA).

2.2 Preparation and characterization of HANPs

HANPs were prepared using a chemical precipitation method. Briefly, $Ca(NO_3)_2$ solution was adjusted to pH 12 by adding concentrated ammonia solution, and $(NH_4)_2HPO_4$ solution (pH 12) was added dropwise during vigorous stirring. A voluminous precipitate was formed. The reaction mixture was gently boiled for 10 min. The precipitate was first allowed to settle and then separated from the supernatant solution. The separated precipitate of HA was washed with distilled water, frozen at –20°C, and lyophilized.

The size of the HANPs was determined by transmission electron microscopy (TEM)(JEM-2010, JEOL Ltd, Japan), and their crystallinity were analyzed by X-ray diffraction analysis (XRD) (BRUKER-AXS, Bruker Co, Germany). The Brunauer–Emmett–Teller (BET) surface area of the HANPs was obtained from the N_2 adsorption-desorption isotherm measured using the Micrometry Tristar system.

2.3 Radiolabeling of BMP-2 with ^{125}I

Radiolabeling was performed according to the iodogen method. Iodogen was dissolved in chloroform at a concentration of 1 mg/ml. Twenty-five microliters of this solution was used to coat the test tube and was subsequently evaporated to dryness. To this tube, 50 μl of a 1 mg/ml solution of BMP-2 and 5 μl of an 18 GBq/ml solution of $Na^{125}I$ were added to initiate the labeling. The mixed solution was incubated and stirred for 30 min at room temperature. Thereafter, Sephadex column chromatography was applied to separate free iodine from the radioactive product. After elution with 0.01 M PBS (pH 7.4) at a flow rate of 1 ml/min for 5 min, the radiolabeled BMP-2 was collected. A combination of paper chromatography using instant thin layer chromatography-silica gel (ITLC-SG), with ethanol/water (85:15 v/v) as the solvent, and radioactivity counting using an γ-counter (Shanghai Institute of Nuclear Instrument Factory, China) were used to identify and analyze the quality of ^{125}I-BMP-2. Free ^{125}I was used as a control to identify the tracer of ^{125}I-BMP-2 on the paper.

2.4 Adsorption of ^{125}I-BMP-2 onto HANPs

Five milligrams of lyophilized HANPs was dispersed in 5 ml of ^{125}I-BMP-2 solution and the solution was stirred at 37°C for 30 min. Upon completion of the adsorption reaction, 1 μl of the resulting solution was extracted for paper chromatography which involved using ITLC-SG with 2.5% bovine serum albumin (BSA) (W/W) in 0.01 M phosphate buffered saline (PBS) (pH 7.4) solution as the solvent, and γ-counter in order to identify the radioactive substance. HANPs absorbed ^{125}I-BMP-2 (HANPs/^{125}I-BMP-2) and ^{125}I-BMP-2 were identified based on the resulting sites of radioactivity on the paper. The amount of ^{125}I-BMP-2 was also determined by the site radioactivity of HANPs/^{125}I-BMP-2 on the paper. The solution was then centrifuged at 4000 rpm for 15 min and the pellet was collected. After washing with water, the pellet was frozen at –20°C and lyophilized. In order to investigate the adsorptive properties of ^{125}I-BMP-2 on HANPs, different concentrations (0–4000 μg/ml) of ^{125}I-BMP-2 solution were used for adsorption.

2.5 In vitro release kinetics of ^{125}I-BMP-2 from HANPs/^{125}I-BMP-2

The in vitro release of ^{125}I-BMP-2 from HANPs/^{125}I-BMP-2 was studied in order to estimate the desorption of ^{125}I-BMP-2 from HANPs/^{125}I-BMP-2. A suspension of HANPs/^{125}I-BMP-2 was prepared under optimized conditions at a concentration of 1 mg/ml in 5 ml of normal saline and incubated at 37°C for 15 days. Each day during the incubation period, the suspension was ultrasonically stirred for 10 min, and the radioactivity and quality of suspension were analyzed by paper chromatography using ITLC-SG with 2.5% BSA (W/W) in 0.01 M PBS (pH 7.4) solution as the solvent, and γ-counter. The release ratio of ^{125}I-BMP-2 from HANPs/^{125}I-BMP-2 was determined based on the percentage of radioactivity at the site of ^{125}I-BMP-2 compared with the total radioactivity on the paper.

3 Results

3.1 Physico-chemical properties of synthesized HANPs

HANPs were prepared using a chemical precipitation method and their physical and chemical properties were determined. In the TEM analysis, the HANPs were observed to be granular-shaped with a diameter of approximately 20 nm (Fig. 1a). The results of BET analysis showed that the specific surface area was 122.48 m^2/g. In the X-ray diffraction analysis, synthesized precipitates exhibited an HA-like pattern (Fig. 1b).

3.2 Identification and analysis of radioactive material

After radiolabeling BMP-2 with ^{125}I, the purity of ^{125}I-BMP-2 was analyzed by paper chromatography using ITLC-SG. The results revealed that ^{125}I moved toward the solvent front (Rf = 0.8) than ^{125}I-BMP-2 (Rf = 0.7) because of the small molecular weight of ^{125}I (Fig. 2). The purity of ^{125}I-BMP-2 was assessed by analyzing the radioactivity at the site of ^{125}I-BMP-2 on the paper. The result showed that the purity of ^{125}I-BMP-2 was >98%. After absorption of ^{125}I-BMP-2 onto the HANPs, the resulting HANPs/^{125}I-BMP-2 was also identified by paper chromatography using ITLC-SG. A typical paper chromatogram pattern of ^{125}I-BMP-2 along with HANPs/^{125}I-BMP-2 was shown in Fig. 3. It was observed that ^{125}I-BMP-2 moved toward the solvent front (Rf = 0.7) while HANPs/^{125}I-BMP-2 remained at the point of spotting (Rf = 0). The results also revealed that the purity of HANPs/^{125}I-BMP-2 was >99%.

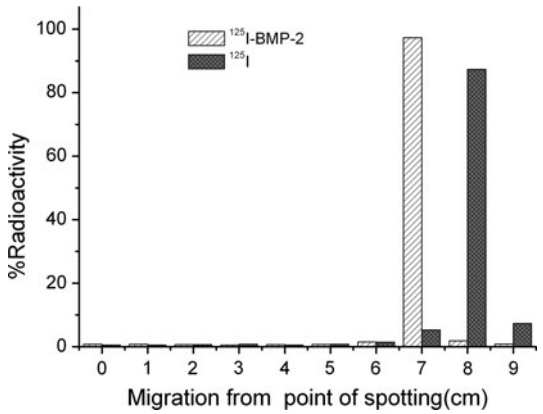

Fig. 2 Paper chromatography patterns of ^{125}I-BMP-2 and ^{125}I using ethanol/water (85:15 v/v) as the solvent

3.3 The amount of ^{125}I-BMP-2 adsorbed on HANPs

The amount of ^{125}I-BMP-2 adsorbed on HANPs was determined according to the results of paper chromatography using ITLC-SG and γ-counter. The adsorptive properties of HANPs were analyzed in the ^{125}I-BMP-2

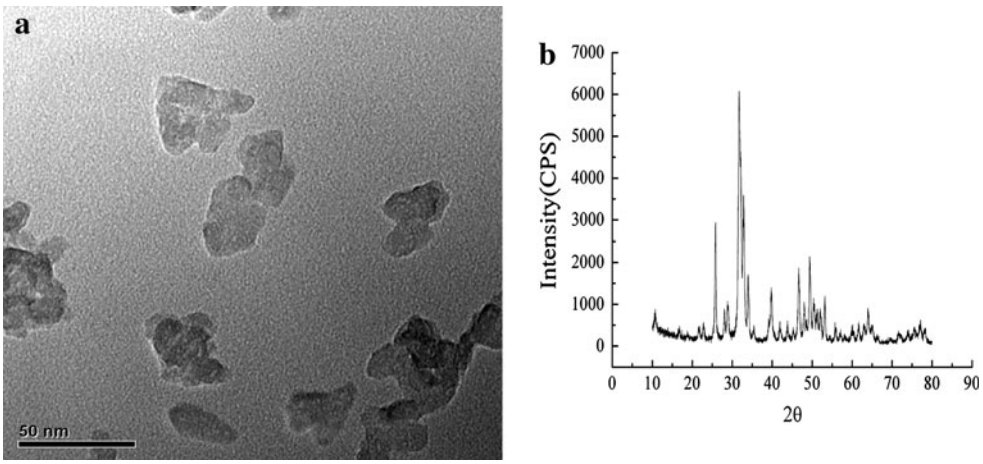

Fig. 1 TEM image (**a**) and XRD pattern (**b**) of HANPs

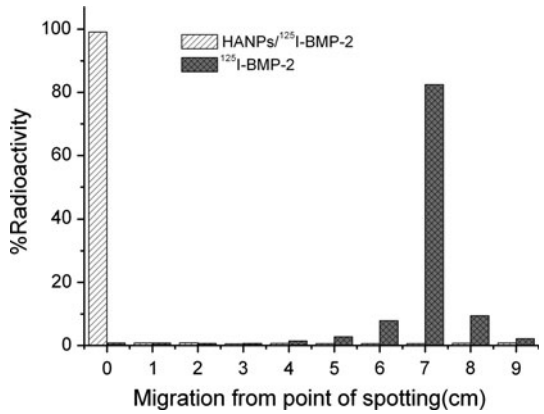

Fig. 3 Paper chromatography patterns of HANPs/^{125}I-BMP-2 and ^{125}I-BMP-2 using 2.5% BSA (W/W) in 0.01 M PBS (pH 7.4) solution as the solvent

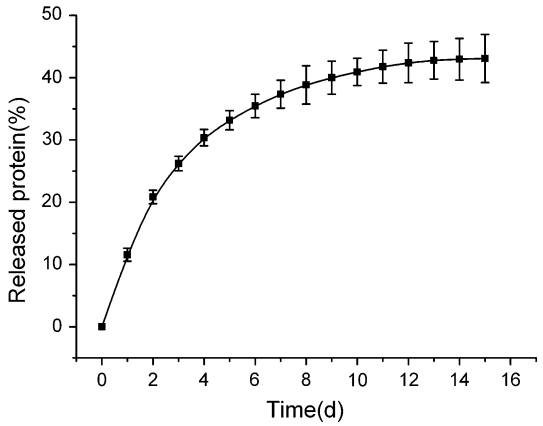

Fig. 5 Release kinetics of ^{125}I-BMP-2 from HANPs/^{125}I-BMP-2. The suspension of HANPs/^{125}I-BMP-2 was prepared under optimized conditions at a concentration of 1 mg/ml in 5 ml of normal saline and incubated at 37°C for 15 days. Each day during the incubation period, the suspension was ultrasonically stirred for 10 min, and the radioactivity and quality of suspension were analyzed

solution at various concentrations. The results showed that the amount of ^{125}I-BMP-2 adsorbed on HANPs increased linearly in the concentration range 31.25–1000 μg/ml ^{125}I-BMP-2 solution and remained constantly at approximately 70 μg/mg in the concentration ranging from 1000 to 4000 μg/ml. The resulting adsorption curve resembled a typical Langmuir curve (Fig. 4).

3.4 In vitro release ratio of ^{125}I-BMP-2 from HANPs/^{125}I-BMP-2

The in vitro release ratio of ^{125}I-BMP-2 from HANPs/^{125}I-BMP-2 was analyzed by employing paper chromatography using ITLC-SG and γ-counter, and was expressed as the percentage of radioactivity at the site of ^{125}I-BMP-2 to the total radioactivity on the paper. Figure 5 showed that the ratio increased linearly from 11.56% on 1 d to 33.16% on 5 d, but thereafter increased moderately to 43.06% on 15 d.

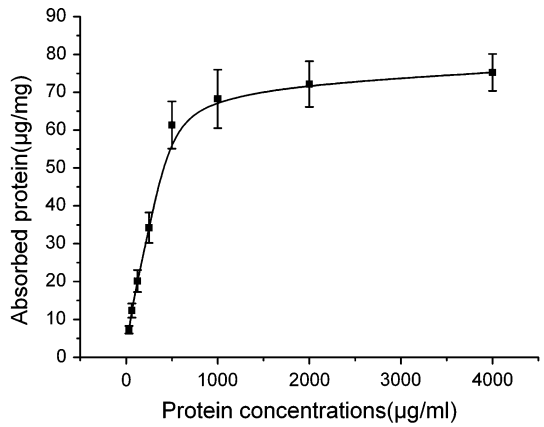

Fig. 4 The chart of the ^{125}I-BMP-2 adsorption on HANPs. 5 mg HANPs was dispersed in 5 ml of ^{125}I-BMP-2 solution in different concentrations (0–4000 μg/ml) and the solution was stirred at 37°C for 30 min

4 Discussion

In this study, HANPs were investigated for their potential to function as a carrier able to absorb and controllably release BMP-2 in vitro. The absorption of BMP-2 on HANPs and the release kinetics of BMP-2 from HANPs were analyzed. The size of HANPs was approximately 20 nm, a small size that made it easy to prepare suspensions of HANPs [20]. This also makes it possible to use paper chromatography instead of centrifugation to separate and identify the components of suspensions of HANPs in BMP-2 solution following adsorption. In order to precisely determine the amount of BMP-2 adsorbed, BMP-2 was radiolabeled with ^{125}I owing to the high sensitivity of radioassay. Paper chromatography using ITLC-SG in conjunction with γ-counter enabled the adsorption efficiency of ^{125}I-BMP-2 on HANPs and the release kinetics of ^{125}I-BMP-2 from HANPs/^{125}I-BMP-2 to be readily analyzed by measuring the radioactivity at the site of each radioactive material. This indicated that the analytical method based on the radiolabeling of ^{125}I was effective for investigating the absorption and release kinetics of small-sized NPs in vitro.

It has been demonstrated that electrostatic attraction is the main mechanism of interaction between HA particles and protein molecules [21, 22], and that electrostatic energy plays a dominant role in the interaction between the

model protein and the HA particle surface [23]. Nanostructure materials that have structural components with at least one dimension in the range of 1 to 100 nm have high surface potential energy due to the small size and high specific surface area [24]. The HA particles used in this study were nanostructured with a diameter of approximately 20 nm (Fig. 1a) and had a specific surface area of about 122 m^2/g. This value was larger than other nanocrystalline HA specific surface area values reported in the literature, and it could result in a higher surface potential energy [25, 26]. This implied that the absorption of proteins onto HANPs and their subsequent release should be efficient.

In order to investigate the adsorptive properties of HANPs with regard to BMP-2, different concentrations (0–4000 μg/ml) of BMP-2 solution were prepared and applied. The results indicated that the amount of BMP-2 adsorbed on HANPs could be as high as 70 μg/mg and that the amount adsorbed was highly correlated with the concentration of the BMP-2 solution. The obtained adsorbance curve resembled a typical Langmuir curve (Fig. 4). This result indicated that the amount of protein adsorbed on HANPs was regulated by the concentrations of protein solution (0–1000 μg/mg). Matsumoto et al. [27] produced a similar adsorbance curve for the absorption of cytochrome *c* on HA microparticles, but that the amount of protein was regulated at approximately only 0–20 μg/mg when using protein solutions in the concentration range 0–200 μg/ml. It could therefore be inferred that the adsorptive efficiency of HANPs was superior to that of HA microparticles when used to absorb proteins. The release kinetics of BMP-2 from HANPs/BMP-2 in the present study was analyzed over 15 days and the results revealed that BMP-2 could be continuously released from HANPs/BMP-2 in vitro (Fig. 5). The release profile was similar to those of PLGA/hydroxyapatite and hydroxyapatite crystals investigated in previous studies [8, 28]. These observations suggested that HANPs should be an effective carrier for sustained release in DDS.

In bone tissue engineering, scaffold materials are routinely employed as carriers to deliver bone growth factors such as BMP-2 and β-TGF. During this process, it is important that the growth factors are continuously released from the scaffold materials [29]. Compared with other scaffold materials, HANPs possess improved mechanical properties and superior bioactivity when used in bone tissue engineering. Furthermore, the HANPs investigated in this study exhibited good absorption and sustained release of BMP-2 over a 15-day period in vitro. This suggest that HANPs as a controlled-release carrier of BMP-2 would be potentially useful as a bone regenerative material.

5 Conclusion

In order to examine the possibility of using HANPs as a controlled-release carrier of BMP-2, this study investigated the absorption of BMP-2 on HANPs and the release kinetics of BMP-2 from HANPs in vitro. It was observed that the amount of BMP-2 adsorbed onto HANPs could be as high as 70 μg/mg and that rate of adsorption was highly correlated with the concentration of BMP-2 solution used. The release profile showed that the release of BMP-2 could be sustained for over 15 days. Collectively, our results suggest that HANPs have the potential to function as a carrier for drug delivery systems and to be applicable as a scaffold material in bone tissue engineering.

Acknowledgments This work was supported by grants from Natural Science Foundation of China (No. 30870680), Science and Technology Commission of Shanghai (No. 0752nm026) and Shanghai Leading Academic Discipline Project (No. S30206).

References

1. Wang X, Li Y, Wei J, de Groot K. Development of biomimetic nano-hydroxyapatite/poly(hexamethylene adipamide) composites. Biomaterials. 2002;23:4787–91.
2. Liao SS, Cui FZ. In vitro and in vivo degradation of mineralized collagen-based composite scaffold: nanohydroxyapatite/collagen/poly(L-lactide). Tissue Eng. 2004;10:73–80.
3. Oonishi H. Orthopaedic applications of hydroxyapatite. Biomaterials. 1991;12:171–8.
4. Yoshikawa H, Myoui A. Bone tissue engineering with porous hydroxyapatite ceramics. J Artif Organs. 2005;8:131–6.
5. Smith GP, Gingrich TR. Hydroxyapatite chromatography of phage-display virions. Biotechniques. 2005;39:879–84.
6. Suen RB, Lin SC, Hsu WH. Hydroxyapatite-based immobilized metal affinity adsorbents for protein purification. J Chromatogr A. 2004;1048:31–9.
7. Doonan S. Chromatography on hydroxyapatite. Methods Mol Biol. 2004;244:191–4.
8. Barroug A, Glimcher MJ. Hydroxyapatite crystals as a local delivery system for cisplatin: adsorption and release of cisplatin in vitro. J Orthop Res. 2002;20:274–80.
9. Vitorino R, Lobo MJ, Duarte J, Ferrer-Correia AJ, Tomer KB, Dubin JR, et al. In vitro hydroxyapatite adsorbed salivary proteins. Biochem Biophys Res Commun. 2004;320:342–6.
10. Mizushima Y, Ikoma T, Tanaka J, Hoshi K, Ishihara T, Ogawa Y, et al. Injectable porous hydroxyapatite microparticles as a new carrier for protein and lipophilic drugs. J Control Release. 2006;110:260–5.
11. Liu Y, Miyoshi H, Nakamura M. Novel drug delivery system of hollow mesoporous silica nanocapsules with thin shells: preparation and fluorescein isothiocyanate (FITC) release kinetics. Colloids Surf B Biointerfaces. 2007;58:180–7.
12. Hughes GA. Nanostructure-mediated drug delivery. Dis Mon. 2005;51:342–61.
13. Du C, Cui FZ, Feng QL, Zhu XD, de Groot K. Tissue response to nano-hydroxyapatite/collagen composite implants in marrow cavity. J Biomed Mater Res. 1998;42:540–8.
14. Sun TS, Guan K, Shi SS, Zhu B, Zheng YJ, Cui FZ, et al. Effect of nano-hydroxyapatite/collagen composite and bone

morphogenetic protein-2 on lumbar intertransverse fusion in rabbits. Chin J Traumatol. 2004;7:18–24.
15. Li C, Vepari C, Jin HJ, Kim HJ, Kaplan DL. Electrospun silk-BMP-2 scaffolds for bone tissue engineering. Biomaterials. 2006;27:3115–24.
16. Boyne PJ, Nakamura A, Shabahang S. Evaluation of the long-term effect of function on rhBMP-2 regenerated hemimandibulectomy defects. Br J Oral Maxillofac Surg. 1999;37:344–52.
17. Heckman JD, Ehler W, Brooks BP, Aufdemorte TB, Lohmann CH, Morgan T, et al. Bone morphogenetic protein but not transforming growth factor-beta enhances bone formation in canine diaphyseal nonunions implanted with a biodegradable composite polymer. J Bone Joint Surg Am. 1999;81:1717–29.
18. Watanabe K, Tsuchiya H, Sakurakichi K, Tomita K. Bone transport using hydroxyapatite loaded with bone morphogenetic protein in rabbits. J Bone Joint Surg Br. 2007;89:1122–9.
19. Jung RE, Weber FE, Thoma DS, Ehrbar M, Cochran DL, Hammerle CH. Bone morphogenetic protein-2 enhances bone formation when delivered by a synthetic matrix containing hydroxyapatite/tricalciumphosphate. Clin Oral Implants Res. 2008;19:188–95.
20. Cho YS, Yi GR, Kim SH, Elsesser MT, Breed DR, Yang SM. Homogeneous and heterogeneous binary colloidal clusters formed by evaporation-induced self-assembly inside droplets. J Colloid Interface Sci. 2008;318:124–33.
21. Gilbert M, Shaw WJ, Long JR, Nelson K, Drobny GP, Giachelli CM, et al. Chimeric peptides of statherin and osteopontin that bind hydroxyapatite and mediate cell adhesion. J Biol Chem. 2000;275:16213–8.
22. Raghunathan V, Gibson JM, Goobes G, Popham JM, Louie EA, Stayton PS, et al. Homonuclear and heteronuclear NMR studies of a statherin fragment bound to hydroxyapatite crystals. J Phys Chem B. 2006;110:9324–32.
23. Shen JW, Wu T, Wang Q, Pan HH. Molecular simulation of protein adsorption and desorption on hydroxyapatite surfaces. Biomaterials. 2008;29:513–32.
24. Brunner TJ, Bohner M, Dora C, Gerber C, Stark WJ. Comparison of amorphous TCP nanoparticles to micron-sized alpha-TCP as starting materials for calcium phosphate cements. J Biomed Mater Res B Appl Biomater. 2007;83:400–7.
25. Ho ML, Fu YC, Wang GJ, Chen HT, Chang JK, Tsai TH, et al. Controlled release carrier of BSA made by W/O/W emulsion method containing PLGA and hydroxyapatite. J Control Release. 2008;128:142–8.
26. Huber FX, Berger I, McArthur N, Huber C, Kock HP, Hillmeier J, et al. Evaluation of a novel nanocrystalline hydroxyapatite paste and a solid hydroxyapatite ceramic for the treatment of critical size bone defects (CSD) in rabbits. J Mater Sci Mater Med. 2008;19:33–8.
27. Matsumoto T, Okazaki M, Inoue M, Yamaguchi S, Kusunose T, Toyonaga T, et al. Hydroxyapatite particles as a controlled release carrier of protein. Biomaterials. 2004;25:3807–12.
28. Chen PH, Tseng YH, Mou Y, Tsai YL, Guo SM, Huang SJ, et al. Adsorption of a statherin peptide fragment on the surface of nanocrystallites of hydroxyapatite. J Am Chem Soc. 2008;130:2862–8.
29. Yamamoto M, Tabata Y, Hong L, Miyamoto S, Hashimoto N, Ikada Y. Bone regeneration by transforming growth factor beta1 released from a biodegradable hydrogel. J Control Release. 2000;64:133–42.